# Surfactants from Itaconic Acid: Physicochemical Properties and Assessment of the Synthetic Strategies

Danilo Malferrari,*,[†] Nicola Armenise,[‡] Stefano Decesari,[§] Paola Galletti,[†,‡] and Emilio Tagliavini[†,‡]

[†]Centro Interdipartimentale di Ricerca Industriale Energia e Ambiente (CIRI), via S. Alberto163, 48123 Ravenna, Italy
[‡]Dipartimento di Chimica "G. Ciamician" Alma Mater Studiorum, Università di Bologna, via Selmi 2, 40126 Bologna, Italy
[§]ISAC−CNR, via P. Gobetti 101, 40129 Bologna, Italy

Ⓢ *Supporting Information*

ABSTRACT: Surfactants are a wide class of compounds used in a broad spectrum of industrial and everyday applications. In this paper, we present the synthesis of a new family of surfactants having C12 and C18 alkyl chains obtained from itaconic acid and fatty amines, molecules industrially obtained from renewable resources. Main physicochemical properties of synthesized surfactants have been measured and their rheological behaviors have been evaluated at the air−water interface using the pendant drop technique. Some of the synthesized surfactants are stimuli responsive compounds, switchable to a polar form in the presence of CO_2. The synthetic strategies have been optimized aiming at the sustainability of the process employing a complete set of green metrics and the software EATOS.

KEYWORDS: Surfactants, Itaconic acid, Sustainable chemistry, Green metrics, Surface properties
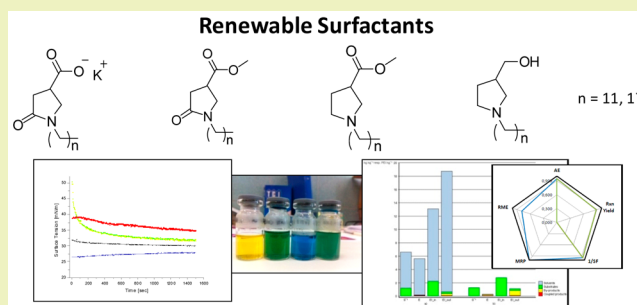
INTRODUCTION

In the last decades, the industrial and research interest in surfactants obtainable from renewable resources has considerably increased. This interest is driven by awareness and concern for the environmental impact of various household products. Moreover, petroleum is a finite resource, the availability of fossil feedstocks in the next future will decrease and its use has adverse effects. Nowadays, the overall market of surfactants is growing at a rate of 3−4% each year and synthetic surfactants cover the majority of the market share.[1] Amphiphiles synthesized from renewable resources represent a commercial alternative to building blocks derived from petrochemical feedstocks.

Recent examples of hydrophilic building blocks for "renewable surfactants" are constituted by carbohydrates, amino acids and polycarboxylic acids. Hydrophobic ones mainly comprise fatty acids, terpenes, sterols and sterols derivatives.

Some nonionic surfactants classes obtained from renewable raw materials are well established, like alkylpolyglucosides (APGs)[2] that are used as self-emulsifiers, as agrochemicals, in personal care products and in pharmaceutical formulations. Despite their popularity, APGs have encountered a variety of synthetic challenges[2] that result in the products being isolated as relatively expensive technical mixtures. Recently, C-glycosides surfactants have been synthesized from carbohydrates through a nonulose intermediate.[3]

Carbohydrates derived from waste biomass, such as 5-hydroxymethylfurfural,[4] furfural,[5] cellulose[6] and sorbitol,[7] have

been proposed as starting materials for surfactants. Nevertheless, some of the compounds listed above come from edible feedstocks and it would be convenient to replace them with nonedible counterparts, such as lignocellulosic biomass.

Recently, the synthesis and biological properties of surfactants incorporating amino acids in the structure have been reported.[8,9] These molecules belong to the group of stimuli responsive amphiphiles:[10] molecules that are responsive to a variety of triggers, including pH, light, magnetic field, CO_2 concentration and redox state.

Another interesting group of surfactants presented in the recent years contains some examples derived from polycarboxylic acids like fumaric acid, itaconic acid (IA) and aconitic acid.[11] In this group, IA has not been fully exploited as building block in surfactants synthesis.[12]

We present a family of surfactants, obtained from fatty amines and IA, that present C12 and C18 alkyl chains. Specifically, fatty amines are industrially produced from fatty acids in three steps through the nitrile process.[13] IA is a naturally occurring compound, non toxic and readily biodegradable;[14] IA is industrially obtained in high yields mainly through biotechnological processes based on fungi of the genus *Aspergillus*, grown on substrates like sucrose, glucose, starch hydrolysates and purified molasses.[15] It is mainly used by

Scheme 1. General Synthetic Routes (A, B and C) to Compounds 1−8
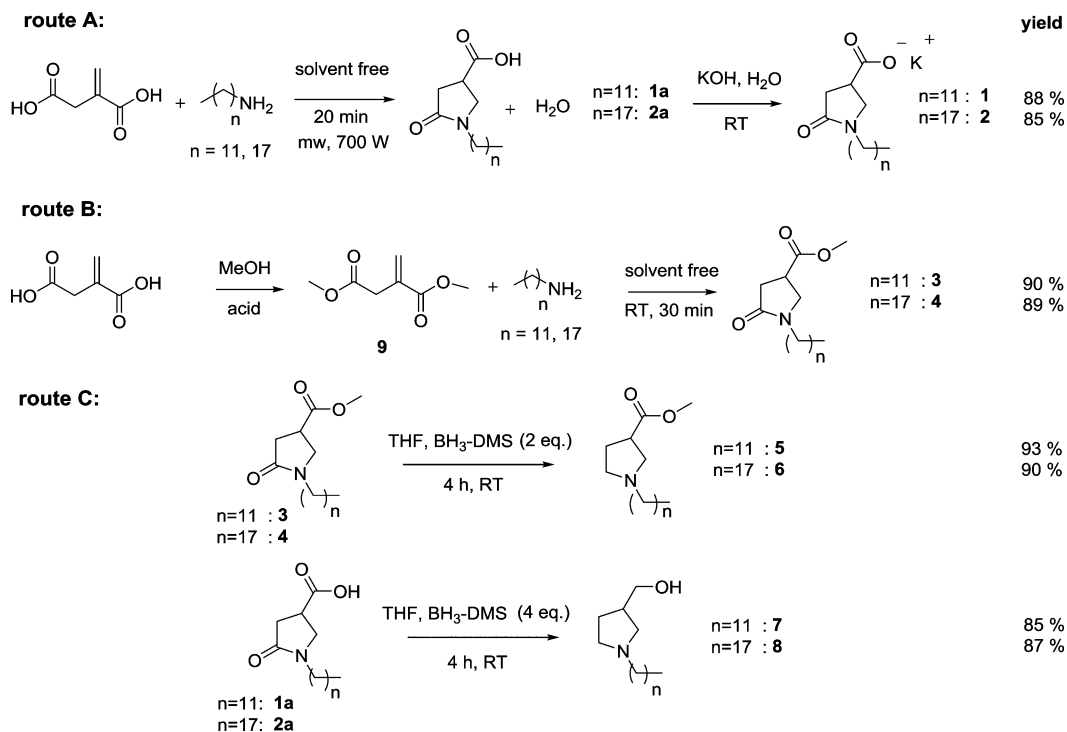
the polymer industry where it is employed as a comonomer for the synthesis of polyesters,[16,17] but it finds applications also in other industrial compounds like additives, detergents, pharmaceuticals and in agriculture. Currently, the total market size involving IA is around 10 000−15 000 t/year.[18]

Herein we report the two step synthesis starting from IA dealing to a new group of surfactants, carrying different functionalities in the polar headgroups; these structural features permit us to design molecules that possess specific physicochemical properties and have the potential to be exploited in micellar organic catalysis and in the soft matter field. In surfactant design, the sustainability of raw materials together with the choice of synthetic strategies are factors of paramount importance;[18] thus, following this ultimate goal, the software EATOS,[19] and a group of green metrics have been used to evaluate the synthetic strategies.[20] The synthetic routes employed have been compared and evaluated looking at the sustainability of the process, solvent and byproducts minimization.

■ RESULTS AND DISCUSSION

Efficient synthetic routes used for the synthesis of compounds 1−8 are represented in Scheme 1. For the complete description of synthetic routes and reaction conditions, refer to Scheme 2 and to the Supporting Information.

The compounds prepared are characterized by a 3-substituted pyrrolidine ring and can be divided into four main groups that belong to different classes of surfactants: anionic (1, 2), nonionic (3, 4) and ionizable (5−8) in water solution. Compounds 1 and 2 bear a 2-pyrrolidone ring and a 3-carboxylic acid or 3-carboxylate functionality depending on pH, compounds 3 and 4 have a 2-pyrrolidone ring with a methyl ester group, compounds 5 and 6 have a pyrrolidine ring and a methyl ester group whereas compounds 7 and 8 have a

pyrrolidine ring and an hydroxymethyl moiety in position three of the ring.

The pyrrolidone scaffold was obtained by conjugate Michael addition of an amine to IA followed by intramolecular spontaneous lactamization between the carboxylic acid in β-position and the secondary amine.

In the literature, the conjugate Michael addition reactions of primary amines to the double bond of IA have been already explored in solvents like toluene and water.[21] Compounds 1a (1-dodecyl-5-oxopyrrolidine-3-carboxylic acid) and 3 (1-dodecyl-5-oxopyrrolidine-3-carboxylic acid methyl ester) have been previously synthesized and tested as transdermal drug delivery agents[22,23] but their interfacial properties have not been reported yet, so a deeper knowledge of their physicochemical properties is desired.

The synthesis of 1a and 2a proceeded smoothly under microwave irradiation, but compounds 3 and 4 have been obtained from dimethylitaconate (9) and the corresponding primary amine in good yields simply by mixing the starting materials and crushing them at RT in a mortar. Compound 9 has been synthesized from IA and methanol both in the presence of Lewis and Brønsted acid catalysts. Compounds 5−8 have been obtained by reducing the lactam functionality of 1a or 2a and the methyl ester group with 2 or 4 equiv of borane dimethylsulfide (BH₃-DMS) respectively, to completely reduce lactam and ester functionalities, optimizing reaction time and product selectivity.

Physicochemical Characterizations. Because of their amphipathic structure in solutions, surfactants tend to form micelles, thermodynamically stable molecular aggregates. The micellar formation takes place above a certain surfactant concentration, the critical micellar concentration (CMC), below which surfactant molecules are present as monomers, above the CMC the free monomers coexist with micellar structures.

Scheme 2. Reaction Schemes of the Synthetic Routes Used for the Synthesis of Compounds 1−4[a]
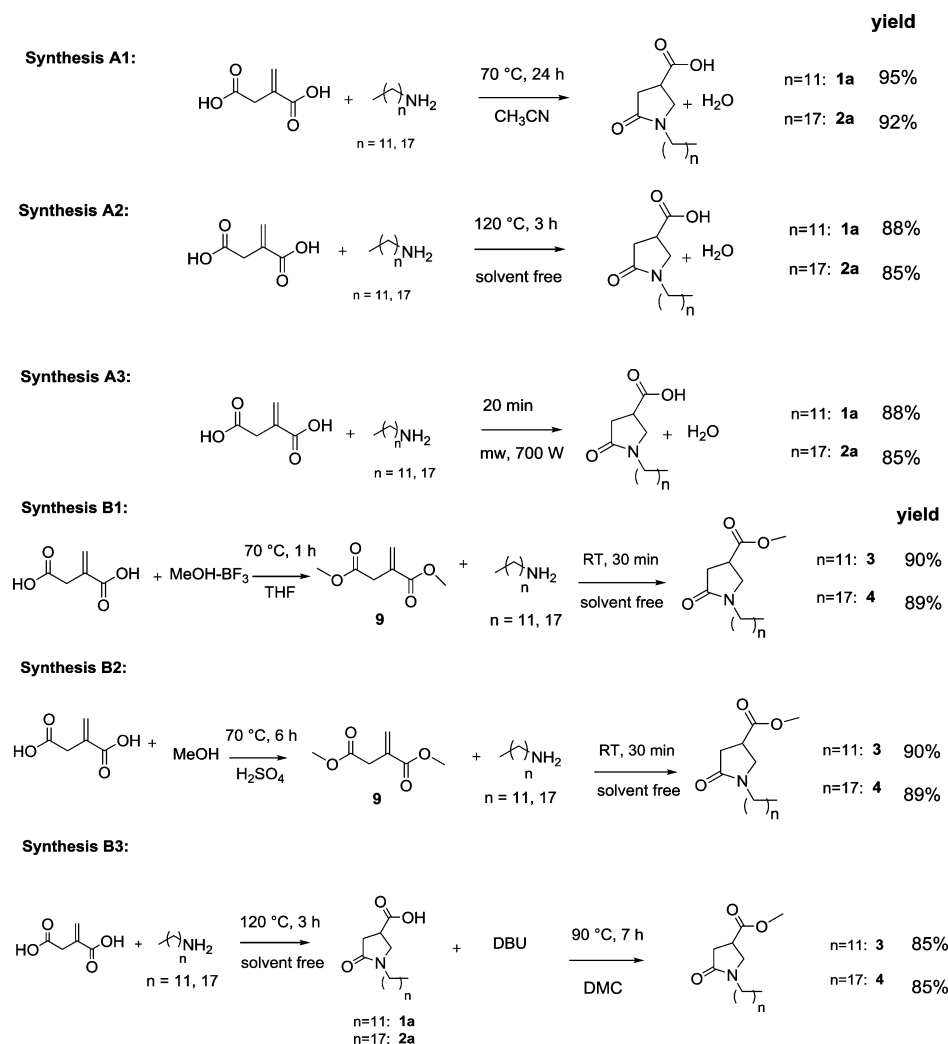
[a]The reaction schemes are representative of the compounds synthesized.

To determine the CMC of **1−8**, three different techniques have been used: two of them exploit the spectroscopic properties of a solubilized dye, the third one examines the behavior of a bulk solution property (conductivity).

We employed two different fluorescent probes: Pyrene (Py) and Nile Red (NR); the structures and steady state fluorescence emission spectra are presented in Figure S21 in the Supporting Information. Py is an hydrophobic molecule and it has been recently proposed to be localized in the hydrophobic interior of the micelles or aggregates,[24,25] under the hydrophilic heads of the molecules. NR in polar media exhibits, owing to its capability to establish H-bonds with protic solvents, a red shift in the emission maximum (λmax −660 nm), together with fluorescence quenching (Figure S21 in the Supporting Information).[26] The CMC values have been also measured by means of conductivity.[27]

Py I_1/I_3 ratio measurements, maximum emission intensities for NR and conductivity data are presented in Figure S22, Figure S23 and Figure S24 in the Supporting Information, respectively; CMC results are summarized in Table 1. CMC values are in the concentration range between 0.1 and 5 mM, in line with values of common surfactants, to give few examples: sodium dodecyl sulfate (SDS, 7.4 mM, see Table 1),

Table 1. CMC Values, Mean Aggregation Numbers, log K_{ow}, log D and pKa Values for Compounds 1−8

compound	CMC[a] [mM]	CMC[b] [mM]	CMC[c] [mM]	N^{agg}[d]	log K_{ow}[e]	log D[e]	pKa[g]
SDS	7.4	8.1	7.2	63			
1	1	5	1	54	4.8	2.0	4.5
2	0.3	0.3	0.3	64	7.0	5.2	4.5
3	0.2	0.1	n.d.	57	4.8 (4.7[f])	5.3	n.d.
4	1.0	1.8	n.d.	68	7.5	8.4	n.d.
5	1.7	1.3	0.8	43	5.9 (5.8[f])	4.4	9.2
6	0.8	0.7	0.4	52	8.6	7.5	9.3
7	0.7	0.6	0.8	57	5.5 (5.3[f])	2.8	10.1
8	0.2	0.5	0.1	60	8.4	6.0	10.1

[a]From Py I_1/I_3 ratio. [b]From NR fluorescence. [c]From conductivity. [d]Value at 25 °C (RT).[30] [e]Predicted using ALOGPS software version 2.1; log D values at pH 7.4.[31−33] [f]Measured with OECD method n. 117, 2004.[34] [g]Predicted using the EPISUITE software.[35]

cetyltrimethylammonium bromide (CTAB, 0.92 mM) and Triton X-100 (0.2−0.9 mM).[28,29]

Compounds **7** and **8**, characterized by an alcohol functionality and a tertiary amine, present the low CMC values in the C12 series as well as in the C18; whereas CMC values of **5** and **6** are the higher of the C12 and C18 series, respectively. CMC values of compounds **3** and **4** (Table 1), which do not present ionizable groups in the molecular structure, are not measurable by means of conductivity, thus the CMC is clearly reported by means of I_1/I_3 ratio and NR.

In Table 1 are also recorded the mean aggregation numbers (N^{agg}) for compounds **1–8**, measured using cetylpyridinium chloride (CPC) as a quencher molecule and Py as a fluorescent probe; SDS, a common anionic surfactant, was used to check the consistency of values.

In Table 1, the estimated log values of the octanol–water partition coefficient (log K_{ow}), the log D values and pK_a values of **1–8** are reported. In the C12 and C18 series, it is visible that the reduction of the amide functionality of the pyrrolidone ring in compounds **5, 7** and **6, 8** is expected to determine an higher degree of lipophilicity, with respect to compounds characterized by the carboxylic (**1** and **2**) and methyl ester functionality (**3** and **4**).

The lower hydrophilicity and solubility in water of compound **4** with respect to **2** is reflected by the log K_{ow} (7.5) and by the log D values. For nonionizable compounds and for compounds characterized by log K_{ow} values lower than 7, corresponding values have also been measured using an OECD method (Figure S25 in the Supporting Information) obtaining values comparable with those previously estimated. Given the pK_a values of these compounds, the pH of the aqueous solutions of compound **1** is acidic, compound **5** and **7** are basic and compound **3** is neutral (Figure S26 in the Supporting Information); titration curves are reported in Figure S27 in the Supporting Information.

The study of surface tension and other surface properties is another important parameter, motivated by the large number of industrial processes involving interfaces, such as coating, detergency, printing and foams.

At the air–water or oil–water interface, above the CMC, the equilibrium surface tension (σ_{eq}) of a surfactant solution is not achieved instantaneously: surfactant molecules must first diffuse from the bulk solution to the interface and then adsorb. For compounds **1–8**, this phenomenon is visible in the surface tension profiles plotted in Figure S26 in the Supporting Information. Compounds **1–8** have been solubilized at concentrations (5 mM) above the CMC values. Each compound presents a different profile, indicating a specific tendency to go at the air–water interface associated with specific kinetics. It is interesting to notice the difference between σ_{eq} values of compound **3** and **4**. Even if **3** and **4** have the same polar headgroup, the difference in the length of the hydrophobic tail is fundamental to determine different kinetics of absorption; compound **4** presents an high lipophilicity, as suggested by high values of log K_{ow} and log D and the lowest value of HLB of the series (according the Davies' method). Lower values of σ_{eq} are achieved with compounds **7** and **8**, which are characterized by quick kinetics of absorption. Compounds **3, 5** and **6** are the ones characterized by slower kinetics to σ_{eq}.

Table 2 summarizes the σ_{eq} values, the elastic modulus (ε) and the effective dilation viscosity (η_d) values for compounds **1–8**. These data have been collected to characterize different types of rheological properties of the surfactant films formed at the air–water interface, because the macroscopic response of

Table 2. σ_{eq}, ε, η_d, HLB and Kt of Compounds 1–8 for 5 mM Solutions

compound	σ_{eq}, surface tension [mN m^{-1}]	ε, elastic modulus [mN m^{-1}]	η_d, viscosity [mN m^{-1}]	HLB^a	Kt [°C]
1	45	36	37	8.6 (27.8)	64
2	39	147	480	6.7 (24.9)	70
3	33	34	151	9.1 (9.1)	48
4	61	31	26	7.2 (6.2)	56
5	35	11	25	8.6 (11.2)	48
6	44	38	149	6.7 (8.4)	68
7	28	11	58	7.4 (10.2)	26
8	30	20	170	5.7 (7.4)	38

^{a}Calculated using the Griffin's and Davies' (between brackets) methods.[36,37]

film properties to surface deformation is inherently linked to fundamental physicochemical properties of surfactants.

Several technological steps in the detergent industry, flotation and sewage disposal are based on the formation of foams of a definite lifetime. The stability or instability of foams and emulsions is to a great extent determined by the surface rheological properties of adsorption layers at the liquid interfaces; for these aspects, the knowledge of dilational elasticity, dilational viscosity and transport effects are important.

Dynamic surface tension measured while variations of the surface area were induced using the pending drop technique. The σ_{eq} values reported in Table 2 are referred to the equilibrium state of the films. Common surface dilatational parameters like ε and η_d were derived by increasing or reducing the volume of the drop, resulting in the expansion or compression of its surface.[38] The σ_{eq} values for compounds **7** and **8** are the lowest in the group of surfactants synthesized. Interestingly, the two compounds alter dramatically the surface tension at the air–water interface. Compound **4**, characterized by a low solubility in the water phase consequently does not change the σ_{eq} to a great extent (61 mN m^{-1} at equilibrium). These data can be explained in terms of poor solubility of compound **4** and reflect its scarce tendency to distribute at the air–water interface. Compound **4** also presents an high CMC value and the minimum decrease in the σ_{eq} can be related to the higher number of molecules that participate to the formation of micellar aggregates. Moreover, the kinetic of absorption at the air–water interface (similarly to compound **3**, Figure S28 in the Supporting Information) is linear for compound **4** and presents a value that is not far from that of pure water surface tension (72 mN m^{-1} at RT).

For three homologues of surfactants couples, **1–2, 5–6** and **7–8**, it can be noted that the ε and η_d values increase moving from compounds that present C12 chains to the compounds having C18 chains. In these cases, the lengthening of the alkyl chain increase the viscoelastic behavior of the water layer at the air–water interface. Increases in ε and η_d values are particularly evident for anionic compounds **1** and **2**, but are also relevant for nonionic compounds **5–6** and for the couple **7–8**, where the difference in σ_{eq} values is not so relevant.

In Table 2 are also reported the hydrophile–lipophile balance (HLB) values calculated for compounds **1–8** using the Griffin's and Davies methods. The HLB of a surfactant is an empirical correlation that measures the tendency to partition between oil and water phase and the value is directly proportional to the surfactants' solubility in water. The Griffin's
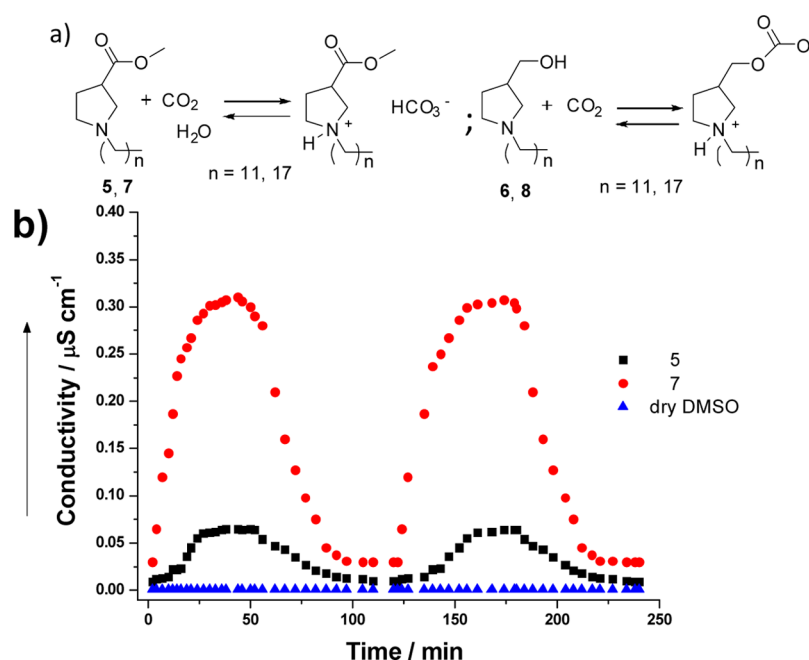
Figure 1. (a) Switching of **5**−**8** in the presence of H_2O and CO_2. (b) Conductivity of DMSO solutions of **5**−**7** as a function of time during two cycles of treatment with CO_2 followed by N_2.

method does not take into account the contribution of highly hydrophilic substituents like carboxylate and sulfonate ones, whereas the Davies' method does. As is predictable, big differences are registered in HLB values of compounds **1** and **2** when measured employing the two different methods.

According to Griffin's HLB values, compounds **1**, **4**, **5** and **7** can be classified as wetting agents; compound **3**, which is nonionic, can be classified as a wetting agent or an oil in water (o/w) emulsifier. Compounds **2**, **6** and **8** present the lower HLB values and are classified as water in oil (w/o) emulsifiers.

In Table 2. Krafft temperature (Kt) values for **1**−**8** are listed. Kt is the temperature at which the solubility of the surfactant monomer becomes equal to the CMC and is generally interpreted as the melting temperature of a hydrated solid surfactant. Kt usually coincides with the temperature of full clarification of the system and above the Kt, micelles begin to form provoking a rapid increase in the solubility of the surfactants (see also Figure S29 in the Supporting Information).

Data clearly show that compounds **1**, **2**, **4** and **6** are characterized by the higher Kt values (around 70 °C). This property undoubtedly limits their applications in certain processes. Therefore, it is desirable to tailor the molecular structure of surfactants or adjust the aqueous environment by introducing inorganic salts to decrease their Kt for practical uses.

Compounds **7** and **8** are the most interesting ones in terms of solubility at low temperatures, the Kt values are present at 26 and 38 °C, respectively.

Compounds **5**−**8** present in their structure two functionalities that allow them to be switched to a polar structure in water phase in the presence of water and CO_2. The tertiary amine can be converted into a quaternary ammonium group and the alcohol functionality converted into a carbonate moiety in the presence of water and CO_2 (Figure 1a). To measure the property of switching polarity, solutions of **5**−**8** at 5 mM in DMSO have been prepared; we chose DMSO solutions thanks

to the good solubility of both amphiphilic molecules and CO_2. Data are presented in Figure 1. Figure 1b shows that the conductivity of DMSO solutions can increase during time in the presence of a CO_2 flux directly bubbled into the solution (for details, see the Experimental Section). The conductivity values, indicative of the presence of the charged form, can be reversibly decreased by removing CO_2 through heating and bubbling an inert gas like nitrogen (N_2) into the solution containing surfactant. It is interesting to note that the increase or decrease in conductivity from bubbling CO_2 is not registered in pure DMSO, indicating that the "switching process" of compounds **5**−**8** needs water (150 μL of H_2O in 3 mL of DMSO), as outlined in Figure 1a. Interestingly, this property can be useful in applications where the increase in surfactant hydrophilicity can decrease its loss into an extracting organic phase.

Assessment of the Synthetic Strategies. Looking for the sustainability of the synthetic processes, we conducted the synthesis of **1**−**8** with three different pathways and we have analyzed the procedures using two complementary types of green metrics: we employed the software EATOS and the worksheet developed by Andraos.[20]

In the Experimental Section, these metrics and their definitions are specified. Interconnections between these parameters were demonstrated by Andraos.[39,40] The variables measured with EATOS are the quantity of substrate used (indicated as S-1); the Environmental Index in input of the reaction (EI input), that measures the resources used and the risk connected with the chemical reaction and the Environmental Index in output (EI output) that measures the toxicology and the eutrophication potential of products and byproducts.

We have decided to limit the green metrics investigation to the synthesis of the lactam surfactants **1**−**4** through conjugate addition of primary fatty amines to IA and its methyl esters, corresponding to the synthetic routes depicted in Scheme 2. Besides the reaction conditions usually employed and shown in
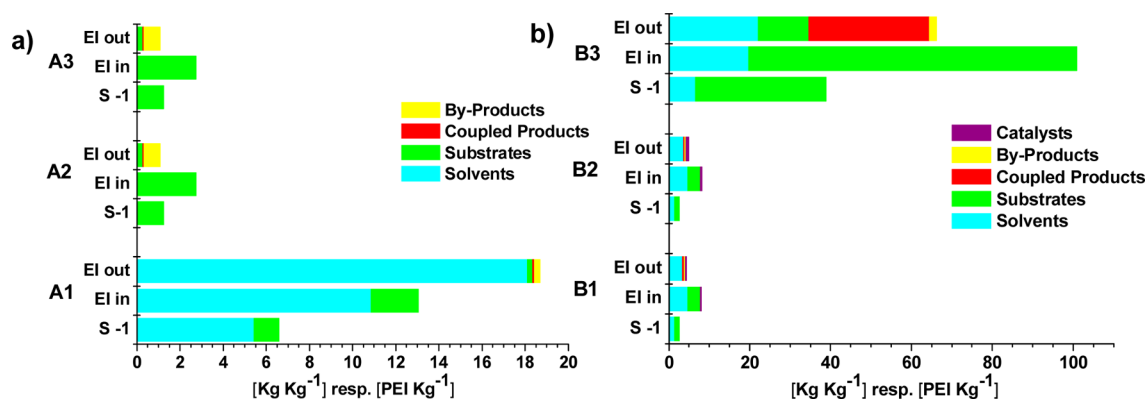
Figure 2. S-1, EI in and EI out values for synthetic routes A1, A2, A3 (a) and B1, B2, B3 (b) investigated with EATOS software.
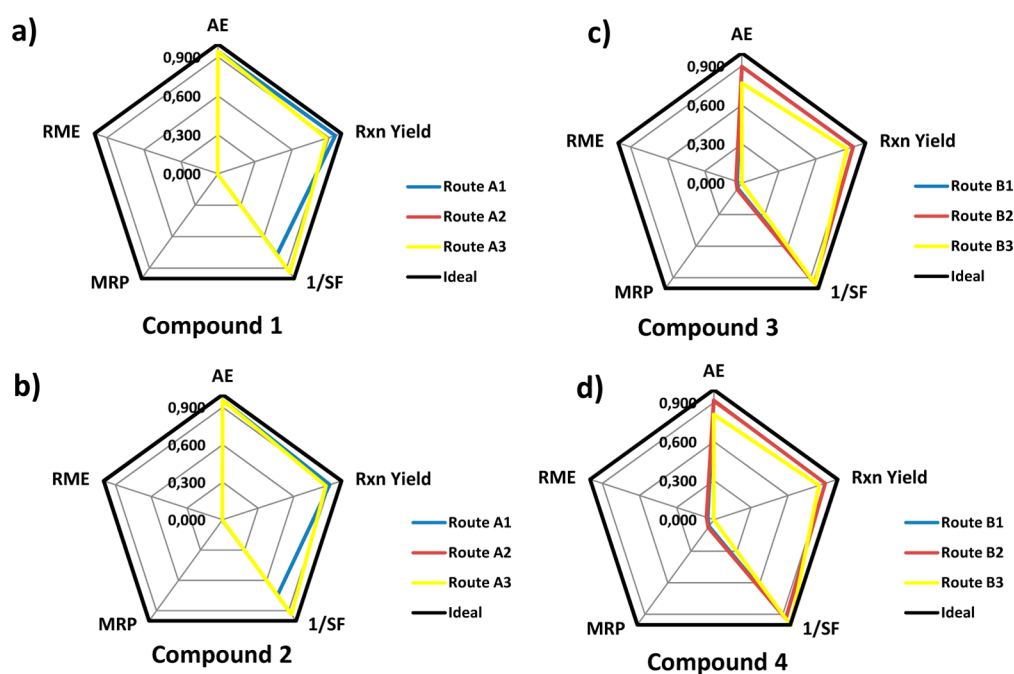

Figure 3. Comparison of the raw material footprint for synthetic routes A1, A2, A3 to compounds **1** (a) and **2** (b); for synthetic routes B1, B2, B3 to compounds **3** (c) and **4** (d).

Scheme 1, here a comparison is performed with other synthetic conditions that also lead to compounds **1–4**. Evaluation of the further elaboration of the lactam moiety goes beyond the aim of the present study. Therefore, the synthetic procedures used for the synthesis of **5–8** will not be taken into account here.

Comparison between the synthetic routes A1, A2 and A3 using EATOS is visible in Figure 2a; comparison between routes B1, B2 and B3 is depicted in Figure 2b. The corresponding numerical values are summarized in Table S1 in the Supporting Information, and summarize the greenness of the processes evaluated following this approach.

Routes A1, A2 and A3 mainly differ in the presence/absence of solvent, in reaction duration, temperature and in the kind of energy input used: external heating with a silicon oil bath (for routes A1 and A2) or a microwave irradiation (for route A3).

Interestingly, routes A2 and A3 provide exactly the same profile, when assessed with EATOS software. However, we should point out that the energy consumption in route A3 is lower than in route A2; indeed, microwaves energy supply to chemical reaction is much more efficient than heat transfer from external heating[41] but this aspect is not taken into account

by the EATOS approach. For A routes, the major impact on S-1, EI input and EI output is due to the solvent. The reactions conducted in solventless conditions (A2 and A3) proved to be more efficient in terms of energy and substrates consumption. We postulate that possible concerns that could arise when solvent free reactions are carried out on a larger scale, like heat release of strongly exothermic reactions, local temperature increase and dishomogeneity,[42] should be of minimal impact in our system, but further investigation will be required before moving to a pilot-plant or industrial scale. A1 and A2 proceed at high temperatures whereas in route B2, dodecylamine and **9** reacted quickly also at 4 °C (mechanically crushing the reagents in a mortar) so a dramatic temperature increase is not expected. Clearly, in view of the scaling up of the solvent free reaction, a deeper understanding of the thermal characteristics is required.

For the synthesis of compounds **3** and **4**, three synthetic procedures have been compared. Routes B1 and B2 exploit dimethylitaconate **9** that is obtained from IA using MeOH-BF$_3$ and H$_2$SO$_4$, respectively. Otherwise, the methylation of the carboxylic acid functionality of **1a** and **2a** in route B3 has been carried out with dimethyl carbonate (DMC) in the presence of

the base 1,8-diazabicyclo[5.4.0]undec-7-ene (DBU). DMC has been chosen because it is considered a green solvent with low toxicity values, it is not classified as a volatile organic compound (VOC)[43] and is a potential green methylating agent. DBU was used as a base because the less expensive and toxic K_2CO_3 or KOH gave rise to the formation of itaconic anhydride only.

Figure 2b shows that route B3 is by far less convenient in terms of solvents consumption, substrates use and byproducts production according to the EATOS evaluation.

It is interesting to notice that the more efficient route is B1, involving the use of MeOH-BF_3 complex instead of H_2SO_4, acid that presents serious health and environmental drawbacks (Scheme 2b and Table S1 in the Supporting Information).

Moving now to the Andraos approach, Figure 3 shows the pentagons that summarize the material footprint for the synthetic routes compared, corresponding numerical values are summarized in Table S2 in the Supporting Information. The synthetic routes A1−B2, with the exception of route B3, are characterized by high levels of reaction yield (Rxn Yield), atom economy (AE) and stoichiometric factor (SF). These data are in agreement with green chemistry principles,[44] which suggest to prefer addition reactions and solventless conditions. With respect to the other two parameters taken into account, MPR and PMI, the assessment through Andraos method is not highly meaningful for processes carried out with typical laboratory methods. Interestingly, as underlined in the worksheets present in the Supporting Information, the values of MRP and PME are low if solvents and materials used in the purification steps are taken into account, independently from the synthetic route considered.

Otherwise, MRP and PME values are high if exclusively measured, considering the amount of solvent used in the synthetic steps (Figure S30 in the Supporting Information). Molar efficiency (ME) values summarized in Table S2 highlight that solvents used during the reactions or in the purification steps have a heavy influence on this metric, rarely highlighted by other metrics. In the synthesis of compounds **3** or **4** is recorded the higher difference in terms of ME, depending on the presence of the solvent. In conclusion, we point out that a complete toxicological characterization such as biodegradability and ecotoxicity of the surfactants has to be assessed to have a complete picture of the toxicological properties and environmental fate of the compounds.

■ CONCLUSIONS

We have reported the two step synthesis of a new class of surfactants derived from IA and fatty amines. The synthetic strategies have been designed for minimizing waste, byproducts and energy consumption. The products obtained constitute an exploitable pool of surface active compounds that thanks to different structures present specific rheological behaviors. Moreover the compounds synthesized can be exploited in reactions of micellar catalysis in water phase.

When assessed through green metrics protocols, reactions conducted in solventless conditions and using microwave devices proved to be efficient and sustainable in terms of toxicity, substrate, solvent and energy consumption. Evaluation of biodegradability and ecotoxicity of the surfactants presented in the present paper, as well as the design of similar surfactants still based on IA, is ongoing in our laboratory.

■ EXPERIMENTAL SECTION

Materials. All reactants were purchased from Aldrich and used without purifications. Aqueous solutions were prepared using Milli-Ro water (resistivity 18.2 MΩ cm at 25 °C; filtered through a 0.22 μm membrane). Flash chromatography was performed on silica gel (230−400 mesh).

Methods and Techniques. *^{1}H NMR and ^{13}C NMR Analysis.* ^{1}H and ^{13}C NMR spectra were recorded on a Varian Mercury 400 spectrometer.

GC−MS Analysis. GC−MS analyses were performed using a 6850 Agilent HP gas chromatograph connected to a 5975 Agilent HP quadrupole mass spectrometer. The GC−MS analysis of compounds **1a**, **2a**, **1**, **2**, **7** and **8** was done by means of silylation.

LC-MS. Analyses were performed on a 1200 series Agilent liquid chromatograph coupled with an electrospray ionization-mass spectrometer (LC-ESI-MS) Quattro Premier XE Waters, using H_2O/CH_3CN as solvents at RT (positive scan, 50−800 m/z).

Elemental Analysis. The elemental composition of the compounds was determined by using an elemental analyzer (Thermo Scientific, Flash 2000, Organic Elemental Analyzer) by means of the flash combustion technique.

FT-IR Spectra. Spectra were measured on a Bruker Alpha FT-IR spectrometer as neat films between NaCl plates and reported in cm^{-1}.

Microwave Reactions. Microwave assisted reactions were performed in a Milestone Mycrosynth equipped with a dual magnetron system with pyramid-shaped diffuser, 1000 W maximum output power, temperature monitor and control via an optic fiber up to 250 °C in the vessel.

Conductivity Measurements. Measurements for the determinations of CMC, Kt and switching properties of **5−8** were carried out with an AMEL 160 conductivitymeter.

Steady-State Fluorescence Measurements. Py and NR steady state fluorescence emission spectra (Figure S21 in the Supporting Information) were acquired with a Jasco spectrofluorometer FP-6200 equipped with a thermostated cuvette holder and a magnetic stirring device.

Biophysical Characterization Techniques. *Critical Micellar Concentration (CMC).* The CMC of **1−8** has been measured using three different techniques: (a) Py I_1/I_3 vibronic ratio measurement. (b) NR fluorescence. The CMC has been measured as stated in the literature.[45] For details, please refer to the Supporting Information. (c) conductivity method. Solutions of **1−8** have prepared in milli-Ro water at different concentrations (0.001, 0.005, 0.01, 0.05, 0.1, 0.5, 1, 5 and 10 mM) and left to stabilize at RT before each measurement. The conductivity meter was previously calibrated with a KCl standard solution of 0.01 M (1.29 mS cm^{-1}). Solutions of **1−8** were placed into a thermostated bath where temperature was maintained constant within ±0.05 °C. The CMC was identified as the intersection point of two approximately linear parts of the conductivity isotherm relating to the premicellar and micellar regions. Each measurement has been carried out in at least three replicates.

Mean Aggregation Number (N^{agg}). The steady-state fluorescence quenching method was used for the determination of N^{agg} at RT.[46] In all experiments, CPC was used as the quencher. Working solutions containing 0.75 μM Py and 5 mM of **1−8** or 10 mM for SDS (above the CMC) were prepared in milli-Ro water. Quencher concentration [CPC] in solution was maintained low enough (0.012 mM) to not perturb the surfactant micelle assembly. The nominal slit widths of excitation and emission were 5 nm, the scan speed was 250 nm min^{-1}. Fluorescence steady-state emission spectra were recorded between 350 and 500 nm using excitation at λ = 334 nm (Figure S21 in the Supporting Information). The micelle N^{agg} was obtained from eq 1:[47]

$$\ln(I_0/I_Q) = (N^{agg} \times [CPC])/([surf] - CMC) \qquad (1)$$

where I_0 and I_Q are the fluorescence intensities of Py in the absence and presence of the quencher CPC, respectively; [surf] is the total concentration of **1−8**, which was kept constant and [CPC] is the concentration of quencher, which was varied (0.00012, 0.0006, 0.0012, 0.006, 0.012 mM). The slope of the linear plots between $\ln(I_0/I_Q)$

versus [CPC] yielded the mean aggregation number (N^{agg}) of the micelles.

Hydrophile–Lipophile Balance Method. HLB values have been measured using the Griffin's and Davies' methods.[36,37]

Krafft Temperature Measurement (Kt). To determine Kt, aqueous solutions of **1−8** (10 mM) and SDS were prepared and placed in a refrigerator at ca. 4 °C for 24 h, where the precipitation of surfactants occurred. The temperature of the precipitated system was raised gradually under constant stirring using a thermostated bath (Heating Immersion Circulator Julabo 13) and its conductance (G, mS) was measured. At each temperature, the conductance reading was checked every 2 min until it reached a steady value.[48]

log K_{ow}, log D, pK_a Prediction. The software Alogps 2.1,[32,33] ECOSAR 1.11 and EPIWEB[34] were employed for the prediction of log K_{ow}, log D and pK_a values of **1−8**. log K_{ow} values have been measured using the OECD method n. 117, 2004.[35]

Colorimetric Changes. 5 mM water solutions of **1**, **3**, **5** or **7** were prepared and 5 drops of bromothymol blue solution were added. The solutions were gently shaken and the colorimetric response observed.

Acid–Base Titration. Titration curves were determined with a pH electrode at RT under a N_2 atmosphere and magnetic stirring. Aqueous surfactant solutions (1.5 mL) of 5 mM were titrated with aqueous NaOH solution of the same concentration. The experiment was twice repeated.

Surface Tension Measurement. Surface tension measurements were performed by a SINTECH PAT1 tensiometer. The σ_{eq} values of **1−8** were measured using solutions (5 mM) of deionized water above the CMC (cfr. with data in Table 2). The σ_{eq} values were determined at RT using the pendant drop method (data are reported in Figure S23 in the Supporting Information). Elastic module ε and viscosity values η_d (Table 2) for each compound have been calculated acquiring dynamic surface tension data.[41]

Elastic module values $|\varepsilon|$ have been calculated using eq 2:

$$|\varepsilon| = -d\sigma/d\ln A \tag{2}$$

Conductivity Measurements of Compounds 5−8. The conductivity of **5−8** (10 mM) in wet DMSO (150 μL of H_2O in 3 mL of DMSO) was measured. CO_2 was bubbled through the solution for 30 min at RT (24 °C). After this step, N_2 was bubbled through the solution and in the meanwhile the temperature was raised to 60 °C for 30 min. The CO_2 and temperature increase cycles were repeated two times (60 and 60 min, respectively). In a control experiment, air was bubbled through the solution of **5** (10 mM) in undried DMSO (3 mL) for 15 min at RT. The conductivity did not rise. CO_2 was then bubbled through for 2 min, causing the conductivity to rise.

ASSOCIATED CONTENT

Ⓢ Supporting Information

^{1}H NMR and ^{13}C NMR spectra, detailed synthetic procedures and characterization data for **1a−8**, Py and NR steady state fluorescence emission spectra, vibronic ratio measurements (I_1/I_3) of Py, CMC of **1−8** using the probe NR, conductivity versus concentrations traces, acid−base titration, photograph of pH indicator/surfactant water solution, surface tension traces, log K_{ow} values and green metrics. The Supporting Information is available free of charge on the ACS Publications website at DOI: 10.1021/acssuschemeng.5b00264.

AUTHOR INFORMATION

Corresponding Author

*Danilo Malferrari. Phone: +39 0544 937353. Fax: +39 0544 937411. E-mail: danilo.malferrari2@unibo.it.

where A is the area of the drop surface and σ_{eq} is the equilibrium surface tension.

Viscosity values η_d have been calculated using eq 3:

$$\eta_d = \varepsilon_0 \omega^{-1} \sin\theta \tag{3}$$

where ε_0 equals the dilatation elasticity modulus $|\varepsilon|$ only for an instantaneous deformation and ω is the angular frequency of the area variation.

Green Metrics. S-1 values, EI in and EI out values have been measured employing the software EATOS v 1.1[19] and a group of metrics described hereby.

The data required for EATOS were obtained from the MSDS downloadable from the Sigma-Aldrich website and from the database of the European Chemical Agency (ECHA).[14] They include: information dealing with risk (R phrases), human toxicity (LD50 oral or dermal, hazard symbols), chronic toxicity (suspect of carcinogen, teratogen, mutagen by International Agency for Research on Cancer - IARC), eco-toxicology (WGK, EC50 48h *Daphnia magna*), biodegradation and accumulation (BCF, log P_{ow}). Prices were taken from the Aldrich catalogue (updated March 2015).

For the calculation of stoichiometric factor (SF), reaction mass parameter (RMP) and the reaction mass efficiency (RME), the spreadsheet produced by J. Andraos[39,40] has been used.

The *E*-factor[50] was calculated as eq 4:

$$E\text{-factor} = \frac{\text{(total waste [kg])}}{\text{(mass of product/s [kg])}} \tag{4}$$

Process mass intensity (PMI) was calculated applying eq 5:[50]

$$PMI = \frac{\text{total mass used in a process or in a step [kg]}}{\text{mass of product/s [kg]}} \tag{5}$$

Molar efficiency (ME)[51] was calculated using eq 6:

$$ME = \frac{\text{moles products}}{\sum(\text{moles starting materials + moles of additives + moles catalyst + moles solvent})} \times 100 \tag{6}$$

Notes

The authors declare no competing financial interest.

■ REFERENCES

(1) Foley, P.; Kermanshahi, A.; Beach, E. S.; Zimmerman, J. B. Derivation and synthesis of renewable surfactants. *Chem. Soc. Rev.* **2011**, *41*, 1499−1518.

(2) von Rybinski, W.; Hill, K. Alkyl polyglycosides - Properties and applications of a new class of surfactants. *Angew. Chem., Int. Ed.* **1998**, *37*, 1328−1345.

(3) Foley, P. M.; Phimphachanh, A.; Beach, E. S.; Zimmerman, J. B.; Anastas, P. T. Linear and cyclic C-glycosides as surfactants. *Green Chem.* **2011**, *13*, 321−325.

(4) Arias, K. S.; Climent, M. J.; Corma, A.; Iborra, S. Biomass-derived chemicals: Synthesis of biodegradable surfactant ether molecules from hydroxymethylfurfural. *ChemSusChem* **2014**, *7*, 210−220.

(5) Gassama, A.; Ernenwein, C.; Hoffmann, N. Photochemical key steps in the synthesis of surfactants from furfural-derived intermediates. *ChemSusChem* **2009**, *2*, 1130−1137.

(6) Puga, A. V.; Corma, A. Efficient production and separation of biodegradable surfactants from cellulose in 1-butyl-3-methylimidazolium chloride. *ChemSusChem* **2014**, *7*, 3362−3373.

(7) Corma, A.; Hamid, S. B. A.; Iborra, S.; Velty, A. Surfactants from biomass: A two-step cascade reaction for the synthesis of sorbitol fatty acid esters using solid acid catalysts. *ChemSusChem* **2008**, *1*, 85–90.

(8) Colomer, A.; Pinazo, A.; García, M. T.; Mitjans, M.; Vinardell, M. P.; Infante, M. R.; Martínez, V.; Pérez, L. pH-sensitive surfactants from lysine: Assessment of their cytotoxicity and environmental behavior. *Langmuir* **2012**, *28*, 5900–5912.

(9) Faustino, M. C.; Calado, A. R. T.; Garcia-Rio, L. Dimeric and monomeric surfactants derived from sulfur-containing amino acids. *J. Col. Interface Sci.* **2010**, *351*, 472–477.

(10) Brown, P.; Butts, C. P.; Eastoe, J. Stimuli-responsive surfactants. *Soft Matter* **2013**, *9*, 2365–2374.

(11) Okada, Y.; Banno, T.; Toshima, Z.; Matsumura, S. Chemoenzymatic synthesis and properties of novel optically active cationics containing carbonate linkages. *J. Oleo Sci.* **2009**, *58*, 519–528.

(12) Tate, B. E. Itaconic acid and derivatives. In: *Kirk-Othmer Encyclopedia*, Wiley VCH: Weinheim, 2000, 865–873.

(13) Svensson M. *Surfactants from Renewable Resources*; Kjellin, M., Johansson, I., Eds.; Wiley VCH: Weinheim, 2010.

(14) http://apps.echa.europa.eu/ (general link for registered chemical substances under REACH regulamentation in ECHA website, for retrieving the substance use the "search for chemicals" menu).

(15) Willke, T.; Vorlop, K.-D. Industrial bioconversion of renewable resources as an alternative to conventional chemistry. *Appl. Microbiol. Biotechnol.* **2004**, *66*, 131–142.

(16) Marvel, C. S.; Shepherd, T. H. Polymerization reactions of itaconic acid and some of its derivatives. *J. Org. Chem.* **1959**, *24*, 599–605.

(17) Lanthong, P.; Nuisin, R.; Kiatkamjornwon, S. Graft copolymerization, characterization, and degradation of cassava starch-g-acrylamide/itaconic acid superabsorbents. *Carbohydr. Polym.* **2006**, *66*, 229–245.

(18) Corma, A.; Iborra, S.; Velty, A. Chemical routes for the transformation of biomass into chemicals. *Chem. Rev.* **2007**, *107*, 2411–2502.

(19) Eissen, M.; Metzger, J. O. Environmental performance metrics for daily use in synthetic chemistry. *Chem.—Eur. J.* **2002**, *8*, 3580–3585.

(20) Andraos, J. Inclusion of environmental impact parameters in radial pentagon material efficiency metrics analysis: Using benign indices as a step towards a complete assessment of "greenness" for chemical reactions and synthesis plans. *Org. Process Res. Dev.* **2012**, *16*, 1482–1506.

(21) Paytash, P. L.; Sparrow, E.; Gathe, J. C. The reaction of itaconic acid with primary amines. *J. Am. Chem. Soc.* **1950**, *72*, 1415–1416.

(22) Sasaki, H.; Kojima, M.; Mori, Y.; Nakamura, J.; Shibasaki, J. Enhancing effect of pyrrolidone derivatives on transdermal drug delivery I. *Int. J. Pharm.* **1988**, *44*, 15–24.

(23) Sasaki, H.; Kojima, M.; Mori, Y.; Nakamura, J.; Shibasaki, J. Enhancing effect of pyrrolidone derivatives on transdermal drug delivery II. Effect of application concentration and pre-treatment of enhancer. *Int. J. Pharm.* **1990**, *60*, 177–183.

(24) Herrenbauer, M. *Biosorption of Polycyclic Aromatic Hydrocarbons (PAH) to Microorganisms and Liposomes*; Shaker Verlag: Aachen, Germany, 2002.

(25) Yan, H.; Cui, P.; Liu, C.-B.; Yuan, S.-L. Molecular dynamics simulation of pyrene solubilized in a sodium dodecyl sulfate micelle. *Langmuir* **2012**, *28*, 4931–4938.

(26) Hungerford, G.; Castanheira, E. M. S.; Real Oliveira, M. E. C. D.; Miguel, M. G.; Burrows, H. D. Monitoring ternary systems of $C_{12}E_5$/water/tetradecane via the fluorescence of solvatochromic probes. *J. Phys. Chem. B* **2002**, *106*, 4061–4069.

(27) Smirnova, N. A.; Vanin, A. A.; Safonova, E. A.; Pukinsky, B.; Anufrikov, Y. A.; Makarov, A. L. Self-assembly in aqueous solutions of imidazolium ionic liquids and their mixtures with an anionic surfactant. *J. Colloid Interface Sci.* **2009**, *336*, 793–802.

(28) Patist, A.; Bhagwat, S. S.; Penfield, K. W.; Aikens, P.; Shah, D. O. On the measurement of critical micelle concentrations of pure and technical-grade nonionic surfactants. *J. Surfactants Deterg.* **2000**, *3* (1), 53–58.

(29) Bielawska, M.; Chodzińska, A.; Jańczuk, B.; Zdziennicka, A. Determination of CTAB CMC in mixed water + short-chain alcohol solvent by surface tension, conductivity, density and viscosity measurements. *Colloids Surf., A* **2013**, *424*, 81–88.

(30) Benrraou, M.; Bales, B. L.; Zana, R. Effect of the nature of the counterion on the properties of anionic surfactants. 1. Cmc, ionization degree at the cmc and aggregation number of micelles of sodium, cesium, tetramethylammonium, tetraethylammonium, tetrapropylammonium, and tetrabutylammonium dodecyl sulfates. *J. Phys. Chem. B* **2003**, *107*, 13432–13440.

(31) VCCLAB, Virtual Computational Chemistry Laboratory, http://www.vcclab.org (accessed March 2015).

(32) Tetko, I. V.; Tanchuk, V. Y. Application of associative neural networks for prediction of lipophilicity in ALOGPS 2.1 program. *J. Chem. Inf. Comput. Sci.* **2002**, *42*, 1136–1145.

(33) Tetko, I. V.; Gasteiger, J.; Todeschini, R.; Mauri, A.; Livingstone, D.; Ertl, P.; Palyulin, V. A.; Radchenkco, E. V.; Zefirov, N. S.; Makarenko, A. S.; Tanchuk, V. Y.; Prokopenko, V. V. Virtual computational chemistry laboratory - Design and description. *J. Comput.-Aided Mol. Des.* **2005**, *19*, 453–463.

(34) OECD Guidelines for the testing of chemicals, section 1, test No. 117: Partition coefficient (n-octanol/water), HPLC Method, 2004.

(35) http://www.epa.gov/opptintr/exposure/pubs/episuite.htm (accessed March 2015).

(36) Griffin, W. C. Classification of surface-active agents by HLB. *J. Cosmet. Sci.* **1949**, *1* (5), 311–326.

(37) Davies, J. T. *Proceedings of 2nd International Congress Surface Activity*; Butterworths Scientific Publications: London, 1957; pp 426–438.

(38) Decesari, S.; Facchini, M. C.; Mircea, M.; Cavalli, F.; Fuzzi, S. Solubility properties of surfactants in atmospheric aerosol and cloud/fog water samples. *J. Geophys. Res.* **2003**, *108* (D21), 4685–4697.

(39) Andraos, J. Unification of reaction metrics for green chemistry: Applications to reaction analysis. *Org. Process Res. Dev.* **2005**, *9*, 149–163.

(40) Andraos, J. Global green chemistry metrics analysis algorithm and spreadsheets: Evaluation of the material efficiency performances of synthesis plans for oseltamivir phosphate (tamiflu) as a test case. *Org. Process Res. Dev.* **2009**, *13*, 161–185.

(41) Polshettiwar, V.; Varma, R. S. Aqueous microwave chemistry: A clean and green synthetic tool for rapid drug discovery. *Chem. Soc. Rev.* **2008**, *37*, 1546–1557.

(42) Correa, W. H.; Edwards, J. K.; McCluskey, A.; McKinnonc, I.; Scott, J. L. A thermodynamic investigation of solvent-free reactions. *Green Chem.* **2003**, *5*, 30–33.

(43) Revision to definition of volatile organic compounds – Exclusion of propylene carbonate and dimethyl carbonate. http://www.epa.gov/ttn/oarpg/t1/fact_sheets/voc_exemp01011309.pdf.

(44) Anastas, P.; Eghbali, N. Green chemistry: Principles and practice. *Chem. Soc. Rev.* **2010**, *39*, 301–312.

(45) Galletti, P.; Malferrari, D.; Samorì, C.; Sartor, G.; Tagliavini, E. Effects of ionic liquids on membrane fusion and lipid aggregation of egg-PC liposomes. *Colloids Surf., B* **2015**, *215*, 142–150.

(46) Turro, N. J.; Yekta, A. Luminescent probes for detergent solutions. A simple procedure for determination of the mean aggregation number of micelles. *J. Am. Chem. Soc.* **1978**, *100*, 5951–5952.

(47) Karukstis, K. K.; McDonough, J. R. Characterization of the aggregates of N-alkyl-N-methylpyrrolidinium bromide surfactants in aqueous solution. *Langmuir* **2005**, *21*, 5716–5721.

(48) Vautier-Giongo, C.; Bales, B. L. Estimate of the ionization degree of ionic micelles based on Krafft temperature measurements. *J. Phys. Chem. B* **2003**, *107*, 5398–5403.

(49) Trost, B. M. Atom economy - A challenge for organic synthesis: Homogeneous catalysis leads the way. *Angew. Chem., Int. Ed.* **1995**, *34*, 259–281.

(50) Jimenez-Gonzalez, C.; Ponder, C. S.; Broxterman, Q. B.; Manley, J. B. Using the right green yardstick: Why process mass intensity is used in the pharmaceutical industry to drive more sustainable processes. *Org. Process Res. Dev.* **2011**, *15*, 912−917.

(51) McGonagle, F. I.; Sneddon, H. F.; Jamieson, C.; Watson, A. J. B. Molar efficiency: A useful metric to gauge relative reaction efficiency in discovery medicinal chemistry. *ACS Sustainable Chem. Eng.* **2014**, *2* (3), 523−532.